

## Estimating site amplification factors from ambient noise

Steven R. Taylor,<sup>1</sup> Peter Gerstoft,<sup>2</sup> and Michael C. Fehler<sup>3</sup>

Received 19 February 2009; revised 28 March 2009; accepted 6 April 2009; published 6 May 2009.

[1] We present a methodology to obtain frequency-dependent relative site amplification factors using ambient seismic noise. We treat a seismic network or array as a forced damped harmonic oscillator system where each station responds to a forcing function obtained from frequency-wavenumber beams of the ambient noise field. A network or array beam is necessary to estimate the forcing function. Taken over long time periods, each station responds to the forcing function showing a frequency-dependent resonance peak whose amplitude and spectral width depends upon the elastic and anelastic properties of the underlying medium. Our results are encouraging in that hard rock sites show little variability and have narrower resonance peaks with reduced amplitudes relative to soft rock sites in sedimentary basins. There is much more variability observed at soft rock sites and a tendency for spectral peaks to shift to higher frequencies and become broader as the site amplification increases. This could be due to lower densities and/or small-strain nonlinearity at stations having high site amplification. **Citation:** Taylor, S. R., P. Gerstoft, and M. C. Fehler (2009), Estimating site amplification factors from ambient noise, *Geophys. Res. Lett.*, 36, L09303, doi:10.1029/2009GL037838.

### 1. Introduction

[2] Most studies of ambient noise have focused on the measurement of interstation group velocities using the time-domain Green's function derived from noise cross correlation [e.g., Gerstoft *et al.*, 2006]. Little work to date has addressed the issue of obtaining attenuation from ambient noise. Recent work of Snieder [2007], Matzel [2008], Prieto and Beroza [2008] and G. A. Prieto *et al.* (Anelastic Earth structure from the coherence of the ambient seismic field, submitted to *Journal of Geophysical Research*, 2008) have begun to address this problem. Snieder [2007] shows that, for acoustic waves in homogeneous anelastic media, correlation-type Green's functions can be correctly estimated, but attenuation is not. In practical applications, however, multiple scattering may aid in recovering attenuation, but the issue remains unresolved. Snieder [2007] also points out the necessity of dividing observed power spectrum by that of the excitation (forcing) power spectrum that we use in our approach. Ambient noise has been used previously for estimating site effects [e.g., Field and Jacob, 1995] by taking the horizontal to vertical spectral ratio to obtain the resonant frequency. The motivation for our work is related to nuclear explosion monitoring, but may have other applications as well, partic-

ularly for seismic hazard studies, calibration of regional arrays and site selection for planned station installations.

[3] In this paper, we describe a simple methodology for estimation of site amplification factors (and possibly relative attenuation) using ambient noise. The approach is to estimate site  $Q$  using standing waves as opposed to taking a propagating wave, tomographic approach [e.g., Matzel, 2008] or the spatial coherency (SPAC) approach of Aki [1957] (e.g., Prieto *et al.*, submitted manuscript, 2008). The idea is to treat time-varying frequency-wavenumber (FK) beams of the ambient noise field as a forcing function beneath a network of stations. Each station responds differently to the forcing function depending on the site structure and attenuation. Differential equations representing different forced, damped harmonic oscillator systems (FDHMO) can be used to estimate  $Q$  and resonance frequencies beneath stations. Additionally, the method does not rely on any time-domain normalization such as 1-bit normalization [e.g., Bensen *et al.*, 2007; Tinsley *et al.*, 2004] that presumably will have a deleterious effect on amplitude measurements necessary for attenuation estimation.

### 2. Data

[4] For our analysis, we collected data for the month of January 2008 from the Southern California Earthquake Data Center (SCEDC) for 72 stations shown in Figure 1a. Stations CHF and BRE are examples of a hard rock and soft rock site, respectively, that will be discussed in subsequent analyses. Data for each station was examined for glitches, dropouts or other irregularities that may make them unsuitable for analysis. The broad-band vertical component (BHZ) data were decimated to 1 Hz prior to processing using appropriate anti-aliasing filters.

### 3. Methodology

[5] Imagine that stations in a network or array are driven by a forcing function derived from the ambient noise field. Each site will respond differently depending upon the elastic and anelastic properties of the underlying medium. As a simple illustration, we use the differential equation for a FDHMO to simulate the response of each station to the forcing function given by [e.g., Lay and Wallace, 1995]

$$\ddot{x} + \gamma\dot{x} + \omega_0^2 x = \frac{1}{m} F(t) \quad (1)$$

where  $F(t)$  is the forcing function,  $x$  is the sensor displacement response to the forcing function,  $\gamma$  is the viscous damping term and  $\omega_0$  is the natural frequency of the oscillator and  $M$  is the mass. The power spectrum of the sensor response is given by

$$P_x(\omega) = \frac{P_F(\omega)/M}{[(\omega_0^2 - \omega^2)^2 + (\gamma\omega)^2]} \quad (2)$$

<sup>1</sup>Rocky Mountain Geophysics, Los Alamos, New Mexico, USA.

<sup>2</sup>Marine Physical Laboratory, Scripps Institution of Oceanography, University of California, San Diego, La Jolla, California, USA.

<sup>3</sup>Department of Earth, Atmospheric and Planetary Sciences, Massachusetts Institute of Technology, Cambridge, Massachusetts, USA.

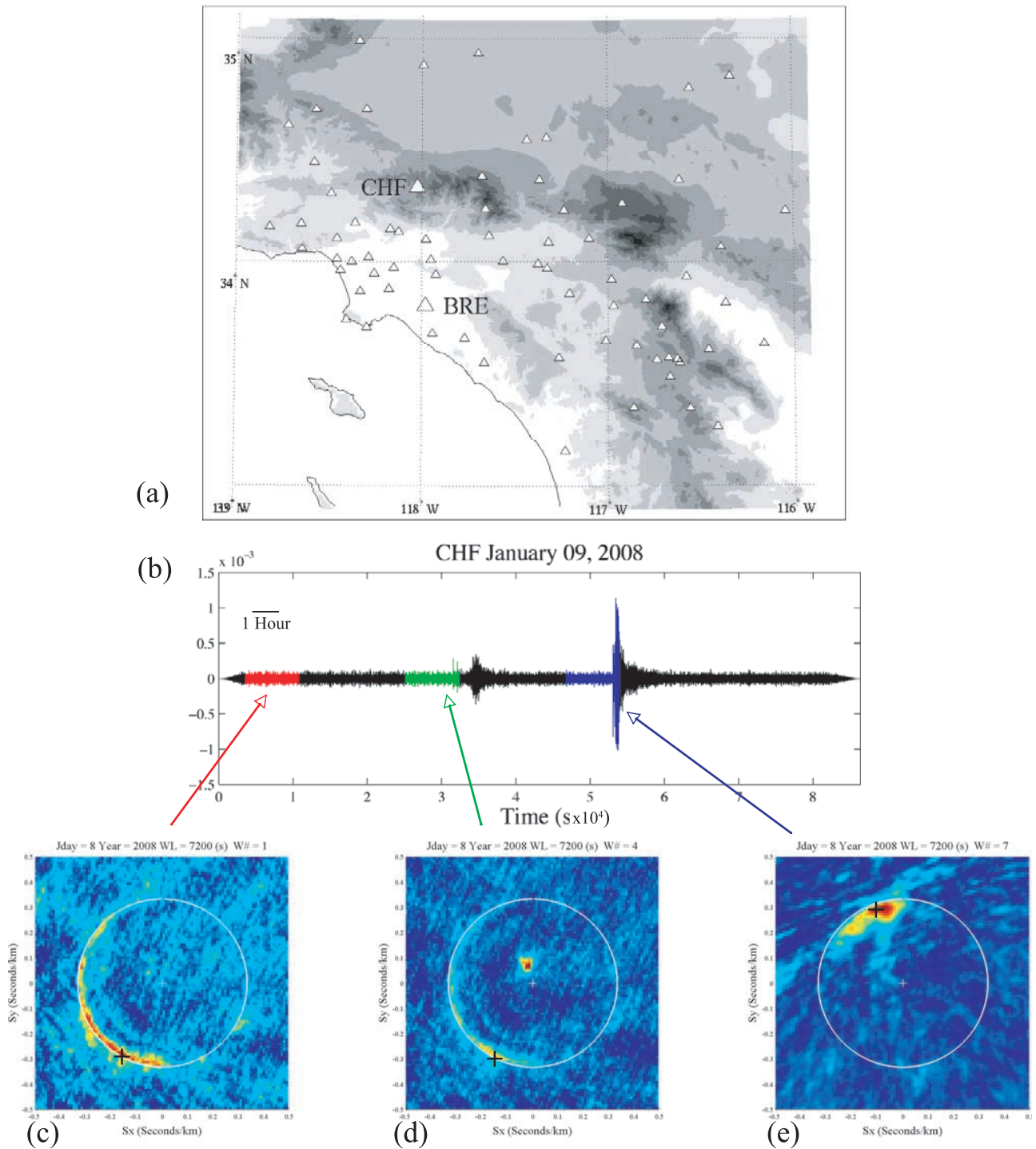


**Figure 1.** (a) Map showing seismic stations of the SCEDC used in this study. CHF and BRE are examples of hard rock and soft rock sites, respectively. (b) One day of BHZ channel data at station CHF for January 9, 2008. (c, d, e) FK beams for three 2-hour samples of noise each with a color-coded arrow indicating the portion of the signal used to compute the beam. White circle corresponds to a phase velocity of 3 km/s and black + symbol to the point at which beam is computed. Note that all available stations for this day shown in Figure 1a were used to compute the FK spectrum.

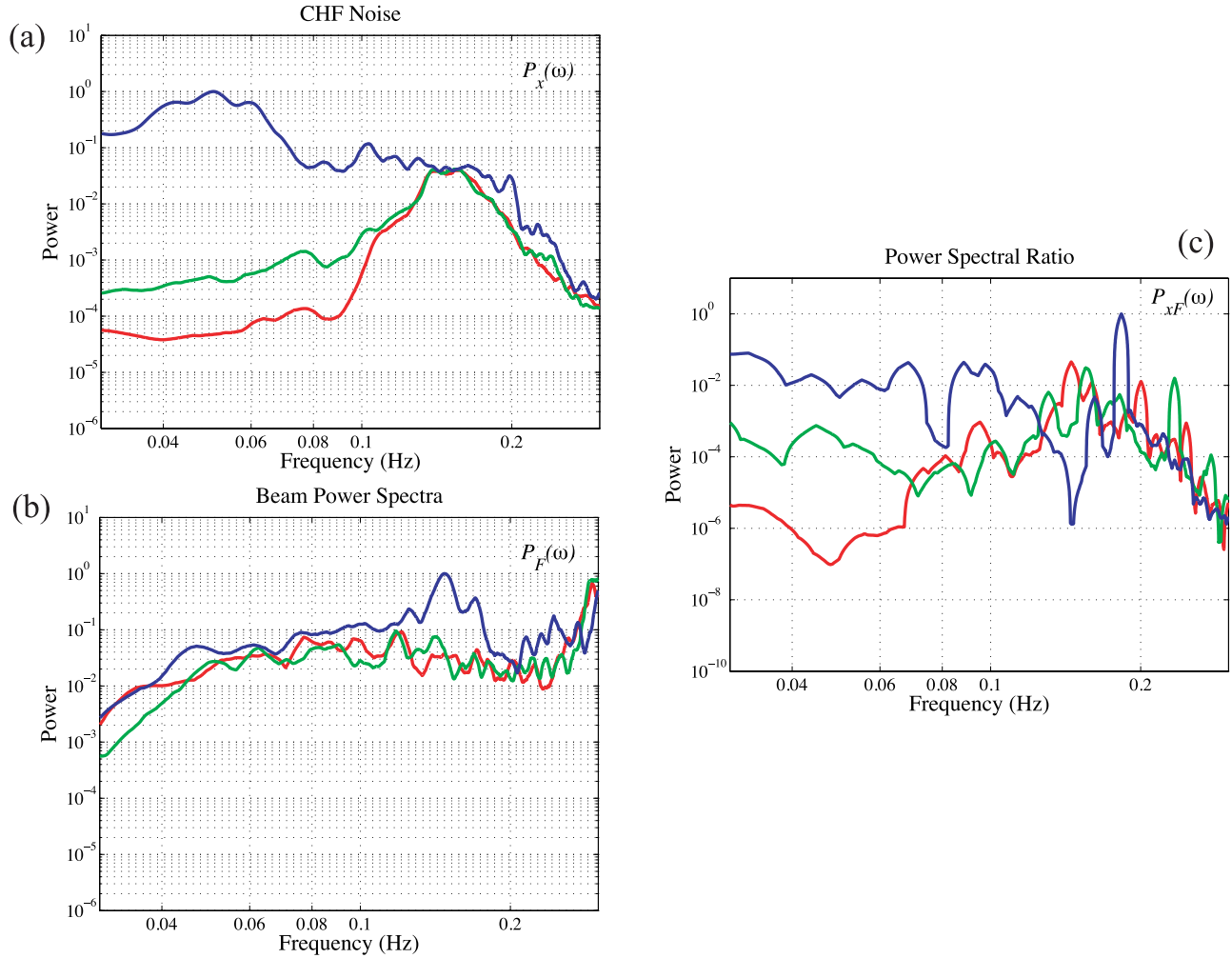


**Figure 2.** (a) CHF single-channel power spectra from noise taken from each of the three windows of Figure 1b using the same color-coding for station CHF as in Figure 1 for the January 9, 2008 noise sample. (b) Smoothed power spectrum for each of the FK beam points shown in Figure 1. (c) Ratio of CHF noise power (Figure 2a) relative to beam power (Figure 2b).

[6] For light damping,  $\gamma \ll \omega_0$ , the resonance peak is narrow and most of the energy is concentrated around  $\omega \approx \omega_0$ . Using the approximation  $(\omega_0 + \omega)(\omega_0 - \omega) \approx 2\omega_0(\omega_0 - \omega)$  the power spectrum for a particular site relative to that of the forcing function is then given by

$$P_{xF}(\omega) = \frac{P_x(\omega)}{P_F(\omega)} = \frac{M}{\omega_0^2 \left[ 4(\omega_0 - \omega)^2 + \left( \frac{\omega}{Q} \right)^2 \right]} \quad (3)$$

where  $\gamma = \omega_0/Q$ . We leave the mass,  $M$ , in the formulation because it will subsequently be related through our observations to the density at each receiver site. Note that the resonant frequency is given by  $\omega_0 = \sqrt{k/M}$  where  $k$  is the spring constant.

[7] For each station, it is then possible to grid search over a range of  $\omega_0$  and  $Q$  values to match the observed resonance peaks. Of course, the single oscillator FDHMO is a very simple system and, as will be seen below, observations suggest that a more complicated representation possibly involving slight nonlinearity may be required.

[8] The power spectrum of the forcing function,  $P_F(\omega)$  in equation (3) is computed from the network or array beam directed towards the maximum power of the ambient noise field. A network or array beam is necessary for estimating the forcing function. This process is illustrated in Figure 1 where we compute the FK spectrum between 0.03 and 0.25 Hz. Figure 1b shows the record at station CHF for January 9, 2008 with three two-hour time windows indicated by red, green and blue. Note that all available stations for this day shown in Figure 1a were used to compute the FK spectrum. Three examples of FK spectra are shown color-coded to time windows on the seismogram in Figure 1b. We compute a beam at the point marked by a + symbol for the maximum power between phase velocities of 2.9 and 3.2 km/s.

[9] The FK spectrum in Figure 1c is typical for a noise sample uncontaminated by signal transients. Figure 1d is contaminated by the arrival of a teleseismic  $P$  wave from the northwest at a high phase velocity although the noise arrivals at relatively lower power can still be seen arriving from the southwest. Restriction of the phase velocities to those between 2.9 and 3.2 km/s allows us to remove the power from the transient  $P$  wave. Figure 1e shows the FK spectrum for a time window that was excluded from our analysis. A large

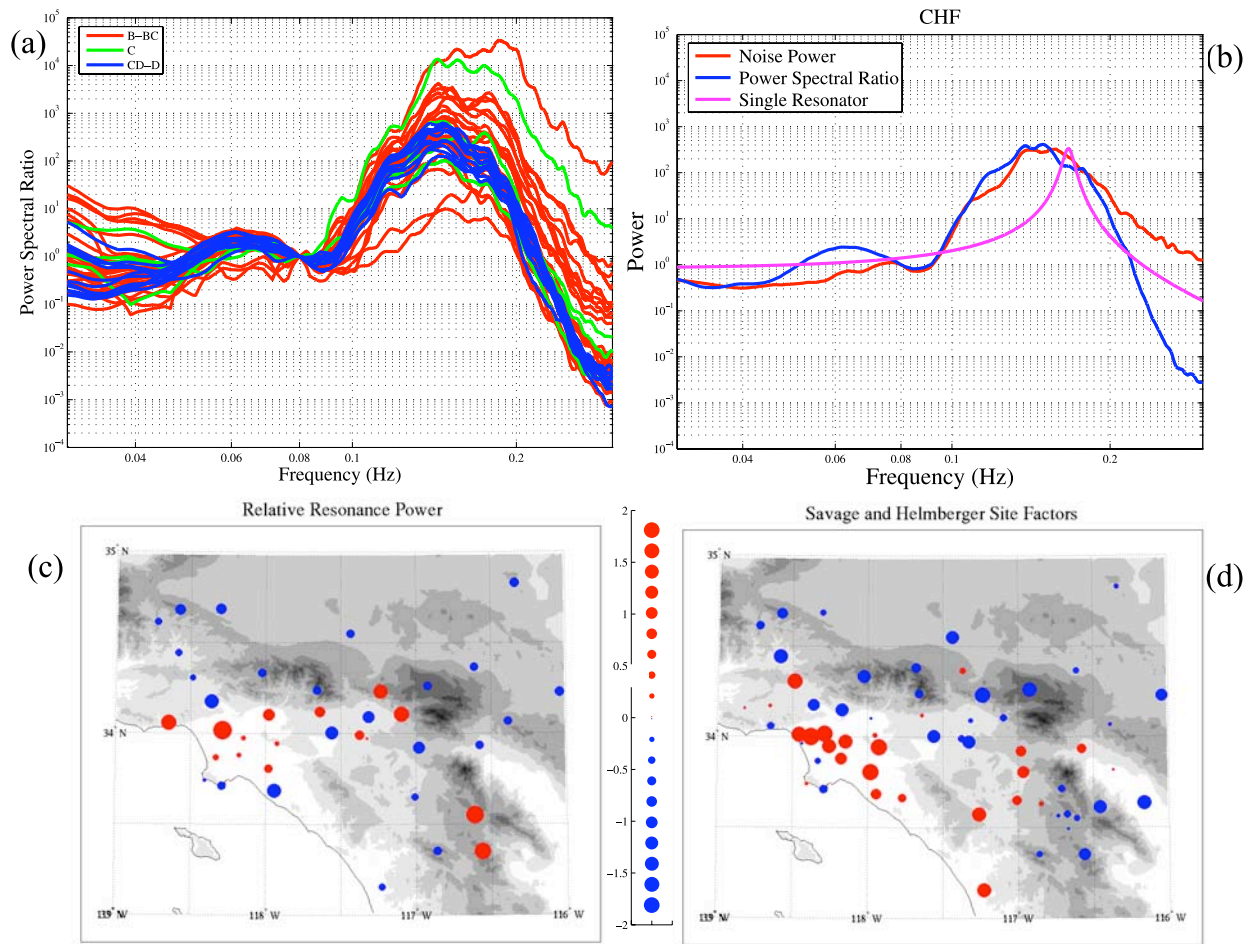


**Figure 3.** (a) Individual power spectral ratio median for all stations with NEHRP site classification factors in three groups all normalized at 0.08 Hz. (b) Station CHF smoothed noise power (red) for sample shown in Figure 2a, power spectral ratio median (blue) and single resonance peak (magenta). (c) Map showing standardized relative resonance power. (d) Standardized logarithm of site amplification terms from *Savage and Helmsberger* [2004]. In both Figures 3c and 3d red indicates larger amplitudes and blue lower amplitudes. Size of symbol is proportional to absolute value of measurement. Frequency axis in Figures 3a and 3b is between 0.03 and 0.3 Hz.

regional surface wave arrives from the northwest at phase velocities similar to ambient noise. It is a simple matter to identify this and eliminate this time window from the analysis. For the month of January, the noise field arrives predominantly from the southwest although a range of azimuths can be observed consistent with *Gerstoft and Tanimoto* [2007]. In practice, a greater sampling of azimuths will help stabilize results and reduce potential directionally-dependent interference effects on the wavefield from multiple sources and lateral heterogeneity. This can be achieved in two ways. The first is by obtaining noise samples over different times of the year. The second is by integrating the FK beam along a semi-circle of azimuth and phase velocity to capture a wider range of ambient noise energy.

[10] Figure 2 shows the processing steps involved with obtaining a site amplification factor from ambient noise for January 9, 2008 shown in Figure 1. We divide the data into two-hour non-overlapping time windows. Figure 2a shows the CHF BHZ power spectrum for each of the noise samples shown in Figure 1b. The power spectrum is computed

from each of the broadband FK beam points using the full array and is shown in Figure 2b. Treating the beam power in Figure 2b as the network forcing function and the individual channel power as the response (Figure 2a), we use the center portion of equation (3) and estimate the site response by computing the power spectral ratio shown in Figure 2c. In our analysis below, we compute the median of the power spectra for each two-hour time segment over all samples passing QC for the month of January 2008 at each station. Note that in Figures 1 and 2 the spectral smoothing is only for illustration purposes and not actually performed until the final processing step.

[11] A number of features are observed in Figure 2. Most notably is the contamination of the third time window by the large regional event arriving from the northwest (as indicated by the FK plot in Figure 1e). The individual channel is strongly affected by this event as well as the power spectral ratio justifying the elimination of this window from subsequent analysis. In contrast, beamforming on the maximum noise power for the second time window effectively removes

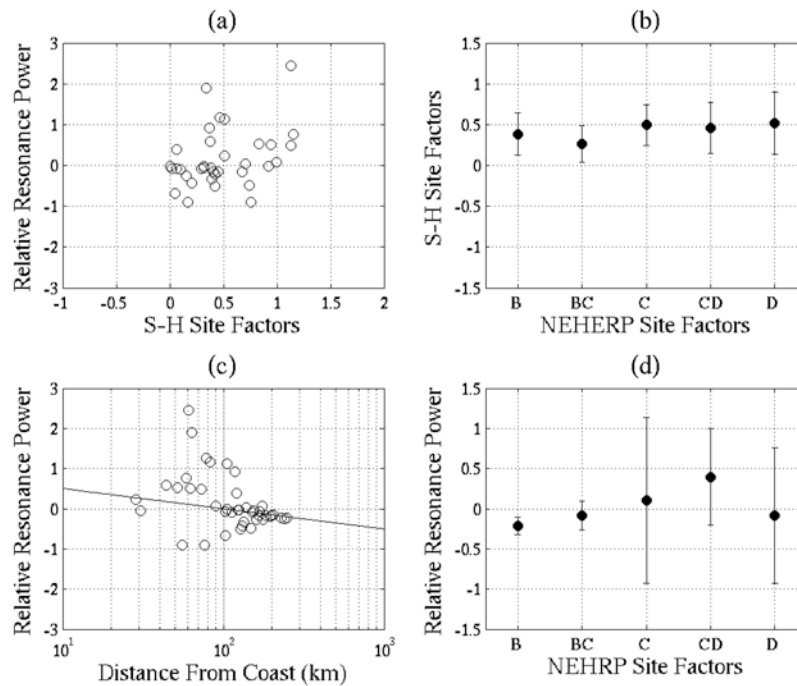


**Figure 4.** (a) Relative resonance power versus logarithm of Savage and Helmberger site factors (S-H, 2004). (b) Median S-H factors with their standard deviation bounds versus NEHRP site factors and. (c) Relative resonance power versus distance from coast (33.5°N, 118.5°W). Black line shows  $r^{-1/2}$  geometrical decay. (d) Median resonance power factors versus NEHRP site factors and one standard deviation.

contamination of the small teleseismic event arriving from the northwest. The beam power shows a different spectral character than that of the individual channel noise. The individual channel noise spectra show a prominent spectral peak at approximately 0.167 Hz as expected for the microseismic noise peak. In contrast, the beam is flatter and has a subsidiary peak at about 0.3 Hz. A histogram of station spacing indicates that spatial aliasing effects for surface waves propagating at 3 km/s may start to occur at frequencies around 0.3 Hz. Thus, our subsequent analysis focuses on frequencies less than 0.3 Hz.

[12] Figure 3a shows individual station power spectral ratio medians (all normalized at 0.08 Hz) grouped by National Earthquake Hazard Reduction Program (NEHRP) site classifications of A. Yong et al. (Geotechnical site characterization in California, the Annual Meeting, 6–11 September 2007, Southern California Earthquake Center, Palm Springs, California; see table at <http://sitechar.gps.caltech.edu/table2.php>). Group B-BC represent soft rock sites, C intermediate, and CD-D hard rock sites. All stations show the same general character with a spectral peak between 0.14 and 0.16 Hz. The hard rock sites (blue) show similar power spectral ratios. In contrast, the soft rock sites show significant variability and there is a tendency for spectral medians to shift to higher frequencies and become broader as the amplitude increases. This could be due either lower density materials at higher amplification sites shifting the resonance frequency to larger values or to slight small-strain nonlinearity for stations having high site amplification [e.g., Assimaki et al., 2008]. Figure 3b shows station CHF smoothed noise power (red) for the noise sample shown in Figure 2c, the power spectral ratio median for January 2008 (blue) and single resonance peak (magenta) computed using equation (3) with a  $Q$  of 20 and

resonance frequency of 0.167 Hz. The shape of the observed spectrum is similar to that of the microseismic noise except that it is narrower and shifted to slightly lower frequencies. This effect is observed for the other stations as well. This suggests that the power spectral peak is indeed a resonance peak driven by microseisms. Obviously, a single resonator model is not the correct representation but has the general character of the observed resonance peak in that the lower frequency power level (where the forcing function and site response are in phase) is greater than that of the high frequency power level (where the forcing function and site response are phase shifted by 180°). More complicated attenuation representations (such as absorption band models) will be required to model the nature of the observed resonance peaks [e.g., Liu et al., 1976].

[13] We compute relative resonance power by normalizing the average of the logarithm of each station power spectral ratio shown in Figure 3a by the median for all stations between 0.08 and 0.3 Hz. Figure 3c shows a map of the standardized,  $Z = (X - \mu_X)/\sigma_X$ , (where  $X$  is the logarithm of the relative resonance power) and Figure 3d the standardized site amplification terms from Savage and Helmberger [2004] who used the  $Pnl$  ratio of vertical to radial energy. In general, there is a good comparison between the relative amplitudes of the observed resonance power and the Savage and Helmberger site factors with larger amplitudes in the basin regions and lower amplitudes in the mountainous terrain. Two stations showing large resonance power located at approximately 33.5° N and 116.5° W correspond to low velocities observed along the San Jacinto fault zone [Hong and Menke, 2006]. There is also a tendency for the observed resonance power to correlate with National Earthquake Hazard Reduction Program (NEHRP) site classifications of

Yong et al. (presented paper, 2007) where soft rock sites have greater amplitudes than hard rock sites as well as a suggestion of narrower spectral width (and lower relative resonance power) at the hard rock sites. These relationships are shown in Figure 4. In general there is a positive correlation between the resonance power and the S-H site factors (Figure 4a). The resonance power and S-H site factors tend to increase with NEHRP site classifications with higher amplification observed for soft rock sites. We also show the relative resonance power as a function of distance from the coast along with a geometrical spreading decay factor of  $r^{-1/2}$  ( $r$  is range in km) that is expected for surface waves propagating from southwest to the northeast (Figure 4c). The fact that we see this geometrical decay from the coast, suggests that a wider sampling of azimuths and improved FK techniques (as previously discussed) will be necessary to capture true site effects.

#### 4. Conclusions

[14] We have developed a standing-wave methodology that has the potential for estimating frequency-dependent site factors for a network or array of stations using ambient noise. The basic idea behind the method is to use the FK beam of the ambient noise field to simulate the forcing function beneath the network. Each site will respond differently to the forcing function depending on the local velocity and attenuation structure. The frequency range of applicability is controlled by the spatial aperture and station spacing used to construct the FK beam. Results using a month of ambient noise data in southern California are encouraging in that the shape and amplitude of individual station resonance peaks appear to correlate with local geology and with site factors of *Savage and Helmberger* [2004]. In general, hard rock sites are characterized by lower amplitude, narrower resonance peaks than those from soft rock sites. There is also a tendency for spectral peaks to shift to higher frequencies and become more asymmetric as the amplitude increases. This could be due to lower densities or to small-strain nonlinearity at stations having high site amplification [e.g., *Assimaki et al.*, 2008].

[15] **Acknowledgments.** This work was sponsored by the Air Force Research Laboratory under contract FA8718-07-C-0005. Data were obtained from the Southern California Earthquake Data Center. We thank Brian

Savage for providing site terms from *Savage and Helmberger* [2004] and Ellen Yu at CalTech for pointing us in the direction of the NEHRP site classifications table of Yong et al. (presented paper, 2007).

#### References

- Aki, K. (1957), Space and time spectra of stationary stochastic waves, with special reference to microtremors, *Bull. Earthquake Res. Inst.*, **35**, 415–457.
- Assimaki, D., W. L. J. Steidl, and J. Schmedes (2008), Quantifying non-linearity susceptibility via site-response modeling uncertainty at three sites in the Los Angeles Basin, *Bull. Seismol. Soc. Am.*, **98**, 2364–2390.
- Bensen, G. D., M. H. Ritzwoller, M. P. Barmin, A. L. Levshin, F. Lin, M. P. Moschetti, N. M. Shapiro, and Y. Yang (2007), Processing seismic ambient noise data to obtain reliable broad-band surface wave dispersion measurements, *Geophys. J. Int.*, **169**, 1239–1260.
- Field, E. H., and K. H. Jacob (1995), A comparison and test of various site-response estimation techniques including three that are not reference-site dependent, *Bull. Seismol. Soc. Am.*, **85**, 1127–1143.
- Gerstoft, P., and T. Tanimoto (2007), A year of microseisms in southern California, *Geophys. Res. Lett.*, **34**, L20304, doi:10.1029/2007GL031091.
- Gerstoft, P., K. G. Sabra, P. Roux, W. A. Kuperman, and M. C. Fehler (2006), Green's functions extraction and surface-wave tomography from microseisms in southern California, *Geophysics*, **71**, S123–S131.
- Hong, T. K., and W. Menke (2006), Tomographic investigation of the wear along the San Jacinto fault, southern California, *Phys. Earth Planet. Inter.*, **155**, 236–248.
- Lay, T., and T. Wallace (1995), *Modern Global Seismology*, Academic, San Diego, Calif.
- Liu, H. P., D. L. Anderson, and H. Kanamori (1976), Velocity dispersion due to anelasticity: Implications for seismology and mantle composition, *Geophys. J. R. Astron. Soc.*, **47**, 41–58.
- Matzel, E. M. (2008), Attenuation tomography using ambient noise correlation, *Seismol. Res. Lett.*, **79**, 358.
- Prieto, G. A., and G. C. Beroza (2008), Earthquake ground motion prediction using the ambient seismic field, *Geophys. Res. Lett.*, **35**, L14304, doi:10.1029/2008GL034428.
- Savage, B., and D. V. Helmberger (2004), Site response from incident  $P_{nl}$  waves, *Bull. Seismol. Soc. Am.*, **94**, 357–362.
- Snieder, R. (2007), Extracting the Green's function of attenuating heterogeneous acoustic media from uncorrelated waves, *J. Acoust. Soc. Am.*, **121**, 2637–2643, doi:10.1121/1.2713673.
- Tinsley, J., S. E. Hough, A. Yong, H. Kanamori, E. Yu, V. Appel, and C. Wills (2004), Geotechnical characterization of TriNet sites, *Seismol. Res. Lett.*, **75**, 505–529.
- M. C. Fehler, Department of Earth, Atmospheric and Planetary Sciences, Massachusetts Institute of Technology, 77 Massachusetts Avenue, Cambridge, MA 02139-4307, USA. (fehler@mit.edu)
- P. Gerstoft, Marine Physical Laboratory, Scripps Institution of Oceanography, University of California, San Diego, 9500 Gilman Drive, La Jolla, CA 92093-0238, USA. (gerstoft@ucsd.edu)
- S. R. Taylor, Rocky Mountain Geophysics, 167 Piedra Loop, Los Alamos, NM 87544, USA. (srt-rmg@comcast.net)